IEEE/CSC SUPERCONDUCTIVITY NEWS FORUM (global edition) January 2015.
This ASC 2014 manuscript 3LPo2I-06 published online in *IEEE Trans. Appl. Supercond.* *(IEEE XPLORE)* DOI: 10.1109/TASC.2014.2377793, on December 5, 2014.

Measurement and Analysis of Critical Current of 100-kA Class Simply-Stacked HTS Conductors

Y. Terazaki, N. Yanagi, S. Ito, Y. Seino, S. Hamaguchi, H. Tamura, T. Mito, H. Hashizume, A. Sagara

***Abstract*—Design activities of the LHD-type helical fusion reactor FFHR-d1 are progressing at NIFS. A 100 kA current capacity is required for the winding conductor under the maximum magnetic field of ~12 T. The high-temperature superconductor (HTS) is a promising option for the helical coil conductor. For the development of such a HTS conductor suitable for the helical fusion reactor, we fabricated 30 kA-class HTS conductor samples, and the excitation tests were successfully carried out. We then fabricated and tested a 100-kA class HTS conductor. The conductor sample is a one-turn short-circuit coil with a race-track shape having a bridge-type mechanical lap joint. The transport current of the sample was induced by changing the external magnetic field, then the critical current of the sample was measured. A numerical analysis of the critical current is being performed by self-consistently solving the spatial distributions of the current density and magnetic field among the simply-stacked HTS tapes to verify the measured critical current of the samples. The critical current characteristics of a single HTS tape is evaluated by the percolation model in the precise analysis.**

***Index Terms*—Critical current, FFHR, fusion reactor, GdBCO, high temperature superconductor.**

I. Introduction

FFHR-d1, the LHD-type helical fusion reactor, requires a 100 kA-class conductor for its continuously wound helical coils having the major radius of 15.6 m and the toroidal magnetic field of 4.7 T [1]. The high-temperature superconductor (HTS) is a promising option as the helical coil conductor. Magnets for fusion reactors using HTS conductors are supposed to have high cryogenic stability and low refrigeration power at elevated temperature operations at >20 K. Furthermore, it was proposed that the helical coils of large-diameter and complex-shape be constructed by connecting conductor segments [2] (or coil segments [3]) exploiting the advantage of HTS. Feasibility studies of the HTS option have been progressing since 2005 [4], [5], then in our previous study in 2012-2013 [6]-[8], we fabricated and tested 30-kA class HTS conductor samples using 20 GdBCO tapes, and measured the critical current of 45 kA at 20 K, 6.1 T and 69 kA at 4.2 K, 1.2 T. In the series of these experiments, the validity of the conductor fabrication, the experimentation and the critical current analysis have been verified for us to proceed into a 100 kA-class HTS conductor testing.

In this study, we fabricated a 100 kA-class HTS conductor sample, which has 54 GdBCO tapes, and measured the critical current. The current was applied to the short-circuit sample by changing the bias magnetic field, and Rogowski coils and Hall probes were used for the current measurements. A numerical analysis of the critical current has been carried out to verify the performance of the 100-kA conductor sample.

This work was supported in part by JSPS KAKENHI, Grant-in-Aid for JSPS Fellows, 26-5370.

Y. Terazaki is with The Graduate University for Advanced Studies, 322-6 Oroshi-cho, Toki 509-5292, Japan (e-mail: terazaki@nifs.ac.jp).

N. Yanagi, S. Hamaguchi, H. Tamura, T. Mito and A. Sagara are with National Institute for Fusion Science, 322-6 Oroshi-cho, Toki 509-5292, Japan (e-mail: yanagi@LHD.nifs.ac.jp).

S. Ito, Y. Seino and H. Hashizume are with Department of Quantum Science and Energy Engineering, Graduate School of Engineering, Tohoku University, 6-6-01-2 Aramaki-Aza-Aoba, Aoba-ku, Sendai, Miyagi, 980-8579, Japan (e-mail: satoshi.ito@qse.tohoku.ac.jp).

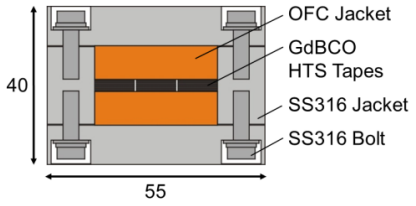

Fig. 1 Illustration of the cross-section of the 100-kA class HTS conductor sample.

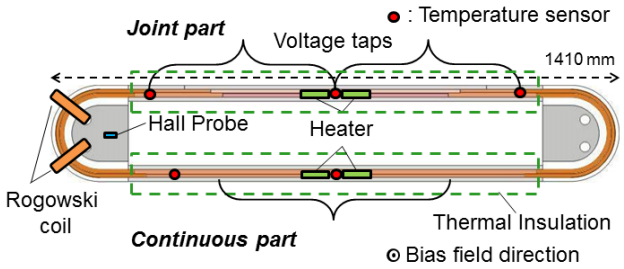

Fig. 2 Schematic view of the overall sample. Locations of voltage taps, temperature sensors, heaters and thermal insulations are indicated.

II. Experimental

A. 100 kA-class HTS conductor sample

Fig. 1 shows a cross-sectional image of the 100 kA-class HTS conductor sample that we fabricated. GdBCO tapes employed in this experiment were produced by Fujikura Ltd. (FYSC-SC10) and has the following layered structure: Hastelloy substrate (100 μm), buffer layers (0.5 μm), GdBCO (2.3 μm), silver (8 μm), tin (2-4 μm) and copper (100 μm). The critical current of the tapes having the width of 10 mm was ~650 A at 77 K, self-field. We used 54 tapes (3-rows and 18-layers) simply stacked in a stabilizing oxygen-free copper

IEEE/CSC SUPERCONDUCTIVITY NEWS FORUM (global edition) January 2015.
This ASC 2014 manuscript 3LPo2I-06 published online in *IEEE Trans. Appl. Supercond.* *(IEEE XPLORE)* DOI: 10.1109/TASC.2014.2377793, on December 5, 2014.

(OFC) jacket without any impregnation or soldering. The copper jacket was then installed in a stainless-steel jacket, which was assembled by bolts. The conductor formed a one-turn short circuit coil with a racetrack shape. The straight sections of the sample were surrounded by a glass-fiber reinforced plastic (GFRP) jacket for thermal insulation as in shown Fig. 2. One of the straight sections has a bridge-type mechanical lap joint (the "joint part") developed in Tohoku University [9], [10] to form the short circuit, while the other side has no joint (the "continuous part"). The tapes were overlapped in a step-wise pattern at the joint part and then the copper side of the tapes was mechanically connected with each other through inserted indium sheets. The details of the joint part and its experimental results are described in [11].

B. Setup

The sample was immersed in liquid helium in the cryostat of the large-scale superconductor testing facility at NIFS. The current was induced in the sample by changing the background magnetic field, which was generated by a 9 T split coil. Voltage taps, temperature sensors and heaters were attached to the stainless-steel jacket as indicated in Fig. 2. Rogowski coils and Hall probes were employed for measuring the current of the short-circuit sample having no current leads [7].

C. Result

Fig. 3 shows the measurement result of the critical current of the 100-kA HTS conductor sample. The continuous part of the sample was heated up to 45 K by using the heaters. The current was induced in the sample by changing the bias magnetic field from 5.6 to 3.9 T. The sample quenched after reaching the maximum current of 68 kA. We note that the sample current evaluated by the Hall probe slightly differs from that by the Rogowski coils during the whole process and the difference becomes distinct especially after the sample reached a critical current. This may be explained by the fact that the Hall probe signal contains the magnetic field generated by the shielding current induced in the HTS tapes, whereas the Rogowski coils do not count this. Thus, we mainly use the current evaluated by the Rogowski coils. We also note that the current evaluated by one of the two Rogowski coils is shown in the figure because the difference of the evaluated current by the two Rogowski coils was within 1%.

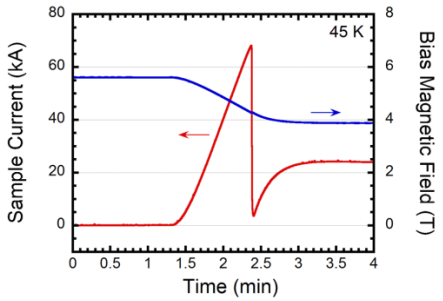

Fig. 3 Waveforms of the sample current and the bias magnetic field at 45 K.

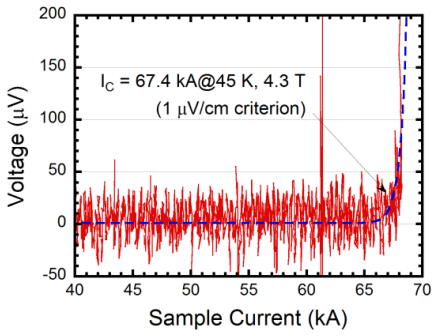

Fig. 4 Voltage waveform of the continuous part of the 100-kA conductor sample as a function of the sample current.

The measured voltage of the continuous part of the sample is shown in Fig. 4 as a function of the sample current for the case with the bias magnetic field of 4.3 T and temperature 45 K. A broken line in the figure is a regression curve expressed by the following equation:

$$V = V_C \left(\frac{I_S}{I_C}\right)^n, \quad (1)$$

where V and V_C are the voltage of the continuous part and the voltage criterion of 20 μV corresponding to the electric field criterion of 1μV/cm times the voltage tap length of 20 cm, respectively. I_S, I_C and n are the sample current, the critical current of the sample determined by the criterion of 1μV/cm and the n value, respectively. The critical current of the sample was evaluated to be 67.4 kA in this case. We also observed the critical current of 72.6 kA at 45 K, 2.8 T.

III. Numerical Analysis of The Critical Current

The critical current of the sample conductor was examined by the following numerical analysis to validate the measurement results of the critical current. In this analysis, the critical current of the conductor sample was calculated using the critical current density of a single HTS tape dependent on the local magnetic field, its orientation and the temperature. In our previous analysis [7], we considered only the local self-field perpendicular to the wide face of the tape. The calculated critical currents were in fairly good agreements with the experimentally observed values. M. Vojenciak *et al.* also performed a similar analysis for Roebel-assembled coated conductor cables, a cross-sectional composition of which is similar to ours, taking account of the dependence of the critical current density on the local self-field and its orientation [12].

A. Calculation Model

Fig. 5 shows the calculation region of this analysis. The bundle of GdBCO tapes is regarded as a one-body conductor, which is divided into 405 elements. The origin of the coordinate is given at the center of the sample. Each element is given an initial current, and the self-field of the sample at each element is calculated by the Biot-Savart's law (the calculation point of the field is at the center of each element). Then, the critical current of each element is evaluated by the magnetic field intensity (= self-field + bias field), its orientation and the sample temperature using the critical current characteristics of a single tape given by the

IEEE/CSC SUPERCONDUCTIVITY NEWS FORUM (global edition) January 2015.
This ASC 2014 manuscript 3LPo2I-06 published online in *IEEE Trans. Appl. Supercond.* *(IEEE XPLORE)* DOI: 10.1109/TASC.2014.2377793, on December 5, 2014.

"percolation model" [13]. If the current of any element exceeds the critical current of that element, the current in that element is reduced to the critical current and the residual current is equally distributed to other elements provided the current is still lower than the critical current in each element. This process is iterated, by developing non-uniform current distribution, until the current of all the elements reaches the critical current. Then, the critical current of the conductor sample is defined as the summation of the current of all the elements.

B. *Critical Current Characteristics of HTS*

The critical current characteristics of the GdBCO tape were evaluated by the percolation model proposed by Kiss *et al.* [13]. The model is a useful method to describe the electric field and current density characteristics of HTS with the scaling of macroscopic pinning force density. The critical current characteristics of HTS are formulated by the following equations:

$$J_C(E_C) = J_{cm} + \left(\frac{m+1}{\rho_{FF}} E_C J_{cm}^m\right)^{\frac{1}{m+1}}, \text{for } B \le B_{GL} \quad (2a)$$

$$J_C(E_C) = -|J_{cm}| + \left(\frac{m+1}{\rho_{FF}} E_C J_0^m + |J_{cm}|^{m+1}\right)^{\frac{1}{m+1}},$$

$$\text{for } B > B_{GL}, \quad (2b)$$

where J_C and E_C are the critical current density and the electric field criterion of 1 μV/cm, respectively. J_{cm} is the threshold value of percolation transition and J_0 corresponds to the half-value width of J_C distribution. The index m is a numerical parameter characterizing the shape of J_C distribution. ρ_{FF} is the flux flow resistivity. B_{GL} is the glass-liquid transition magnetic field, defined as the field when J_{cm} becomes zero. Additionally, the dependence on the orientation of the magnetic field of the critical current characteristics is defined as follows:

$$J_C(B,\theta) = J_C\big(B \cdot f(\theta)\big), \quad (3a)$$

$$f(\theta) = \sqrt{\cos^2\theta + \frac{1}{\gamma}\sin^2\theta}, \quad (3b)$$

where θ is the angle between the direction of the local magnetic field and the axis perpendicular to the wide face of the tape (the c-axis of the GdBCO lattice), and γ is the effective electron mass anisotropy parameter. All the necessary parameters for the critical current characteristics of the GdBCO tape were found in [14] and [15].

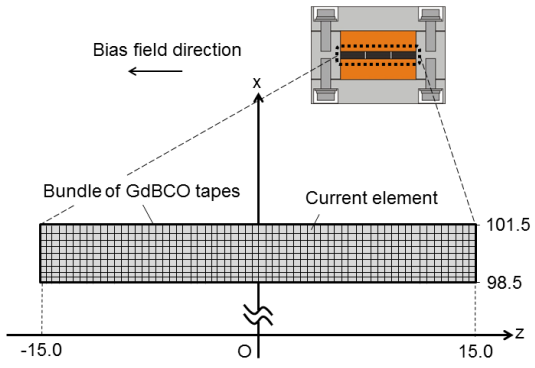

Fig. 5 Schematic illustration of the model of the critical current analysis. The units of the *x*- and *z*-axis are in millimeter.

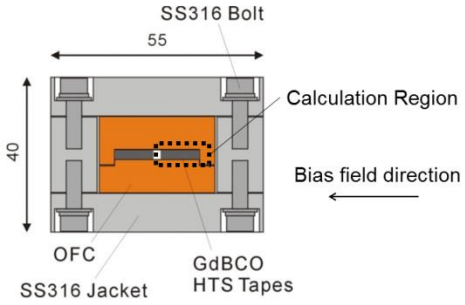

Fig. 6 Cross-sectional illustration of the 30-kA class HTS conductor sample.

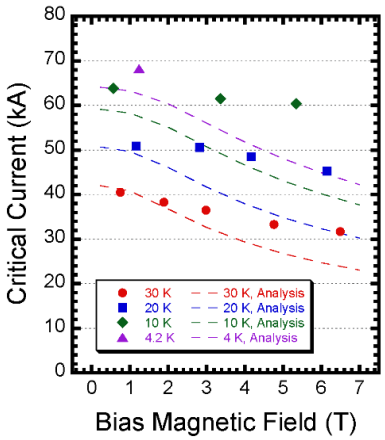

Fig. 7 Critical currents of the 30-kA sample obtained by the experiment and numerical analysis as a function of the bias magnetic field at each temperature. Symbols and curves show the results of the experiment and the analysis, respectively.

C. *Validations of experimental results by numerical analysis for 30 kA-class HTS conductor sample*

The validation of the above mentioned model was performed for the experimental results for 30-kA class HTS conductor sample [7]. An illustration of cross-section of the 30-kA conductor sample having 20 GdBCO tapes (2-rows and 10-layers) is shown in Fig. 6. We note that the calculation region of the 30-kA sample is the cross-section of a row of GdBCO tapes, whereas that of 100-kA sample is the whole cross-section of the tapes.

Fig. 7 shows the critical currents of the 30-kA sample obtained by the experiment and numerical analysis as a function of the bias magnetic field at each temperature. Symbols and curves in the figure show the results of the experiment and the analysis, respectively. The experimental and the analytical results are in fairly good agreement at the lower field region, whereas there is a discrepancy between the both results at the higher field region. This may be due to the difference of the critical current characteristics of the GdBCO tape used in the experiment and the analysis. Figs 8 and 9 show the spatial distributions of the magnetic field and the critical current density in the 30-kA sample at self-field and 6.1 T, respectively. The magnetic field perpendicular to the wide face of the tape (parallel to the c-axis of the GdBCO

IEEE/CSC SUPERCONDUCTIVITY NEWS FORUM (global edition) January 2015.
This ASC 2014 manuscript 3LPo2I-06 published online in *IEEE Trans. Appl. Supercond.* *(IEEE XPLORE)* DOI: 10.1109/TASC.2014.2377793, on December 5, 2014.

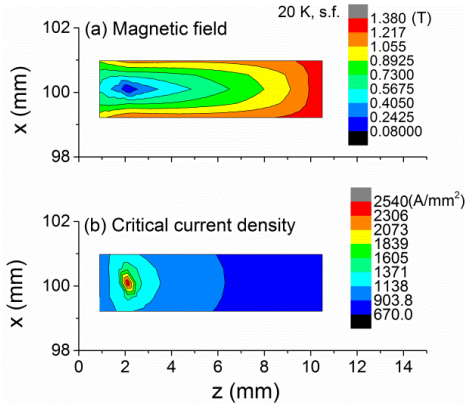

Fig. 8 Distributions of (a) the magnetic field and (b) the critical current density in the 30-kA sample at 20 K, s.f.

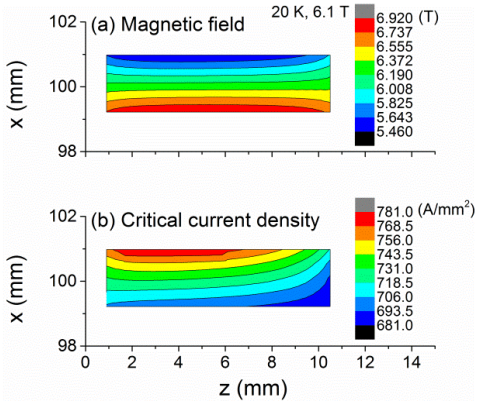

Fig. 9 Distributions of (a) the magnetic field and (b) the critical current density in the 30-kA sample at 20 K, 6.1 T.

lattice) mainly affects the critical current in the self-field case, whereas that of parallel to the wide face of the tape mainly affects in the 6.1 T case. From this, the cause of the discrepancy is considered to be the difference of the critical current characteristics. We will examine this in our future work. The experiment obtained for the critical current characteristics of GdBCO tape will be performed in the near future.

D. Calculation Results for 100-kA class HTS conductor

The critical current analysis for the 100-kA sample was performed. Fig. 10 shows the distributions of the magnetic field and the critical current density in the 100-kA sample at 4.2 K, 0.45 T. In this case, the critical current of the 100-kA sample is evaluated to be 119 kA. The sample current of 118 kA was experimentally observed at 4.2 K, 0.45 T as shown in Fig. 11 without having a quench. Thus, it was confirmed that the 100-kA sample did not show a premature quench, and we consider that the performance of the HTS conductor with simple stacking of tapes was satisfactorily demonstrated in this experiment.

IV. Summary

A 100 kA-class HTS conductor sample as a prototype conductor for the helical fusion reactor was fabricated by

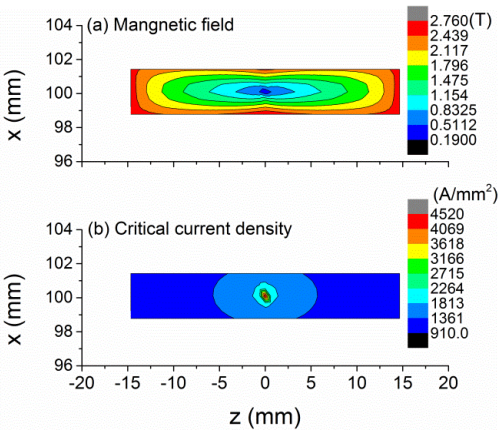

Fig. 10 Distributions of (a) the magnetic field and (b) the critical current density in the 100-kA sample at 4.2 K, 0.45 T.

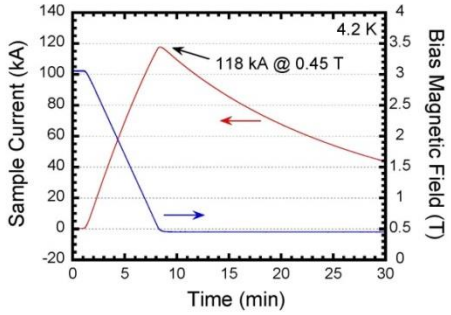

Fig. 11 Waveforms of the current in the 100-kA sample and the bias magnetic field at 4.2 K when the current reached the maximum current of 118 kA.

simply stacking GdBCO tapes. The current was induced in the short-circuit sample by changing the bias magnetic field. The critical current of 67.4 kA and 72.6 kA were measured at the bias magnetic field of 4.3 T and 2.8 T, respectively, at the temperature of 45 K. The 100 kA current was maintained for 1 hour at 4.2 K, and the sample current reached 100 kA at 5.3 T, 20 K and 118 kA at 0.45 T, 4.2 K (reported elsewhere).

A numerical analysis of the critical current of the sample was performed by solving self-consistently the spatial distribution of the magnetic field and current density in the sample. The calculated values for the 30-kA sample agrees well with the experimentally obtained values at the lower field region, whereas there is still some discrepancy at the higher field region. This may be caused by the difference of the critical current characteristics of the tape used in the experiments and the analysis, and the details will be investigated in our future studies. As a result of the analysis for the 100-kA sample, it was confirmed that the sample did not show a premature quench. Thus, we consider that the performance of the sample was satisfactorily demonstrated in this experiment.

Acknowledgment

The authors would like to thank S. Imagawa, K. Takahata and S. Takada for their valuable comments. Special thanks are given to G. Bansal and H. Noguchi.

REFERENCES

[1] A. Sagara, H. Tamura, T. Tanaka, N. Yanagi, J. Miyazawa, T. Goto, R. Sakamoto, J. Yagi, T. Watanabe, S. Takayama, and The FFHR design group, "Helical reactor design FFHR-d1 and c1 for steady-state DEMO," *Fusion Eng. Des.*, vol. 89, pp. 2114–2120, October 2014

[2] N. Yanagi, T. Mito, R. Champailler, G. Bansal, H. Tamura, and A. Sagara, "Design progress on the high-temperature superconducting coil option for the heliotron-type fusion energy reactor FFHR," *Fusion Sci. Technol.* vol. 60, pp. 648-652, Aug. 2011

[3] H. Hashizume, S. Ito, K. Yagi, S. Kitajima, "Proposal of mechanically jointed superconducting magnet using high critical temperature superconductors," *Fusion Eng. and Des.*, vol. 63-64, pp. 449-454, 2002

[4] G. Bansal, N. Yanagi, T. Hemmi, K. Takahata, T. Mito, and A. Sagara, "High-Temperature Superconducting Coil Option for the LHD-Type Fusion Energy Reactor FFHR," *Plasma and Fusion Res.*, vol. 3, p. S1049, Feb. 2008

[5] Y. Terazaki, N. Yanagi, S. Tomida, H. Noguchi, K. Natsume, T. Mito, S. Ito, H. Hashizume, and A. Sagara, "Measurement of the Joint Resistance of Large-Current YBCO Conductors," *Plasma and Fusion Res.*, vol. 7, p. 2405027, Feb. 2012

[6] N. Yanagi, Y. Terazaki, S. Ito, K. Kawai, Y. Seino, T. Ohinata, Y. Tanno, K. Natsume, S. Hamaguchi, H. Noguchi, H. Tamura, T. Mito, H. Hashizume, and Akio Sagara, "Progress of the Design of HTS Magnet Option and R&D Activities for the Helical Fusion Reactor," *IEEE Trans. Appl. Supercond.*, vol. 24, Issue. 3, p. 4202805, June 2014

[7] Y. Terazaki, N. Yanagi, S. Ito, K. Kawai, Y. Seino, T. Ohinata, Y. Tanno, K. Natsume, S. Hamaguchi, H. Noguchi, H. Tamura, T. Mito, H. Hashizume, and A. Sagara, "Critical Current Measurement of 30 kA-Class HTS Conductor Samples," *IEEE Trans. Appl. Supercond.*, vol. 24, Issue. 3, p. 4801305, June 2014

[8] S. Ito, K. Kawai, Y. Seino, T. Ohinata, Y. Tanno, N. Yanagi, Y. Terazaki, K. Natsume, S. Hamaguchi, H. Noguchi, H. Tamura, T. Mito, A. Sagara, and H. Hashizume, "Performance Evaluation of the Mechanical Bridge Joint for 30 kA Class HTS Conductor Samples," *IEEE Trans. Appl. Supercond.*, vol. 24, Issue. 3, p. 4602305, June 2014

[9] S. Ito and H. Hashizume, "Transverse Stress Effects on Critical Current and Joint Resistance in Mechanical Lap Joint of a Stacked HTS Conductor," *IEEE Trans. Appl. Supercond.*, vol. 22, p. 6400104, June 2012

[10] K. Kawai, S. Ito, Y. Seino, N. Yanagi, H. Tamura, A. Sagara, and H. Hashizume, "Optimization of a Mechanical Bridge Joint Structure in a Stacked HTS Conductor, " *IEEE Trans. Appl. Supercond.*, vol. 23, no. 3, p. 4801704, June 2013

[11] S. Ito, Y. Seino, N. Yanagi, Y. Terazaki, A. Sagara, and H. Hashizume, "Bridge-type mechanical lap joint of a 100 kA-class HTS conductor having stacks of GdBCO tapes, " *Plasma and Fusion Res.*, vol. 9, p. 3405086, April 2014

[12] M. Vojenciak, F. Grilli1, S. Terzieva, W. Goldacker, M. Kovacova, and A. Kling, "Effect of self-field on the current distribution in Roebel-assembled coated conductor cables," *Supercond. Sci. Technol.*, vol. 24, p. 095002, July 2011

[13] T. Kiss, M. Inoue, S. Egashira, T. Kuga, M. Ishimaru, M. Takeo, T. Matsushita, Y. Iijima, K. Kakimoto, T. Saitoh, S. Awaji, K. Watanabe, and Y. Shiohara, "Percolative Transition and Scaling of Transport E–J Characteristics in YBCO Coated IBAD Tape," *IEEE Trans. Appl. Supercond.*, vol. 13, no. 2, p. 2670, June 2003

[14] M. Inoue, R. Fuger, K. Higashikawa, T. Kiss, S. Awaji, M. Namba, K. Watanabe, Y. Iijima, T. Saitoh, and T. Izumi, "In-Field Current Transport Properties of 600 A-Class GdBa2Cu3O7-δ Coated Conductor Utilizing IBAD Template," *IEEE Trans. Appl. Supercond.*, vol. 21, no. 3, p. 3206, June 2011

[15] M. Inoue, T. Kiss, D. Mitsui, T. Nakamura, T. Fujiwara, S. Awaji, K. Watanabe, A. Ibi, S. Miyata, Y. Yamada, and Y. Shiohara, "Current Transport Properties of 200 A-200 m-Class IBAD YBCO Coated Conductor Over Wide Range of Magnetic Field and Temperature," *IEEE Trans. Appl. Supercond.*, vol. 17, no. 2, p. 3207, June 2007